Society of Antiquaries of Scotland

Darkness Visible

The Sculptor's Cave, Covesea, from the Bronze Age to the Picts

Ian Armit and Lindsey Büster

ISBN: 978-1-908332-17-2 (hardback) • 978-1-908332-23-3 (PDF)

Armit, I and Büster, L 2020 *Darkness Visible: The Sculptor's Cave, Covesea, from the Bronze Age to the Picts*. Edinburgh: Society of Antiquaries of Scotland. https://doi.org/10.9750/9781908332233

Society of Antiquaries of Scotland is a registered Scottish charity number SC 010440. Visit our website at www.socantscot.org or find us on Twitter @socantscot.

Chapter 4

CHRONOLOGY: ARCHAEOLOGY, RADIOCARBON DATING AND BAYESIAN MODELLING

DEREK HAMILTON, IAN ARMIT, RICK SCHULTING AND LINDSEY BÜSTER

4.1 Introduction

4.1.1 General

Although radiocarbon dating had been planned as part of the Shepherds' work in 1979 and despite some charcoal samples having been packaged for potential submission, no dates were obtained prior to the reanalysis of the human remains in 2006 (Armit et al 2011). Chronological understanding of the site sequence thus remained firmly focused on the presence of diagnostic artefacts. Consequently, Ian Shepherd's final published statement on the site's chronology identified a period of Late Bronze Age activity 'between around 1000 and 800 BC', based on the presence of diagnostic copper alloy bracelets and 'an event in the Sub-Roman Iron Age defined by the deposition of a quantity of fourth-century bronze coins and a series of Pictish pins' (2007: 194). Human activity relating to the intervening centuries, from the Early Iron Age to the Roman Iron Age, was thus entirely unsuspected.

4.1.2 Radiocarbon dates

A total of 51 dates are now available for the site (illus 4.1; table 4.1) and these form the basis for the chronology of the site as now understood. Twenty-four of these dates were obtained as part of the re-examination of the human remains in 2006/7 (Armit et al 2011) and 26 as part of the present programme. The final date was obtained as part of a wider programme investigating ancient DNA of individuals from prehistoric Scotland (Armit et al 2016). With the exception of an initial measurement done at the ^{14}CHRONO facility at Queen's University Belfast, all AMS radiocarbon measurements were undertaken at the Scottish Universities Environmental Research Centre (SUERC).

4.1.3 Sample selection and strategy: 2006/7

The initial dating programme in 2006/7 focused on contextualising the human remains from the Benton and Shepherd excavations (although most of the human skeletal material recovered during Sylvia Benton's excavations has been lost, with the exception of a series of cervical vertebrae showing evidence for decapitation; box section 4). Samples for AMS dating were taken from 11 human bones: 5 of the cut-marked vertebrae from Benton's excavations; 3 juvenile mandibles, a child's frontal with indications of post-mortem modification and an immature thoracic vertebra, all from the Shepherds' excavations; and a tibia fragment, showing signs of peri-mortem trauma, which was found in 2006 eroding from Benton's spoil heap immediately outside the cave. One of the mandibles (SF312) and the frontal (SF231) failed to provide dates.

In addition, a selection of mammal bones was identified from stratified deposits from the Shepherds' excavations (the charred cereal grain assemblage, which would have been preferable for dating, could not be traced at that time, although it was subsequently recovered in the course of work for the present post-excavation programme; see section 4.1.4 below). These were selected from a range of contexts in the East Passage to provide an indication of the chronological range of the entrance deposits, as well as to enable a proper assessment of the degree to which human remains were 'fresh' at the time of their deposition. Bone was selected from large and medium terrestrial mammals. Although only one sample derived from articulated bone (SUERC-16593), the material was generally well preserved, with good surface integrity. Sample selection focused on large elements less likely to have moved through stratigraphic layers. Where possible, only one bone from each species (cattle, sheep/goat, pig/boar) was selected for any given context so as to avoid the possibility of duplicating an individual from the same layer. A sample from the articulated dog burial in the uppermost surviving layers of the West Passage appeared to represent the latest stratigraphically datable sample from the 1979 excavations.

4.1.4 Sample selection and strategy: 2015

A further series of 26 samples was submitted in 2015 to enable the construction of a chronological model for deposition in the West Passage and to refine the existing model for the East Passage.

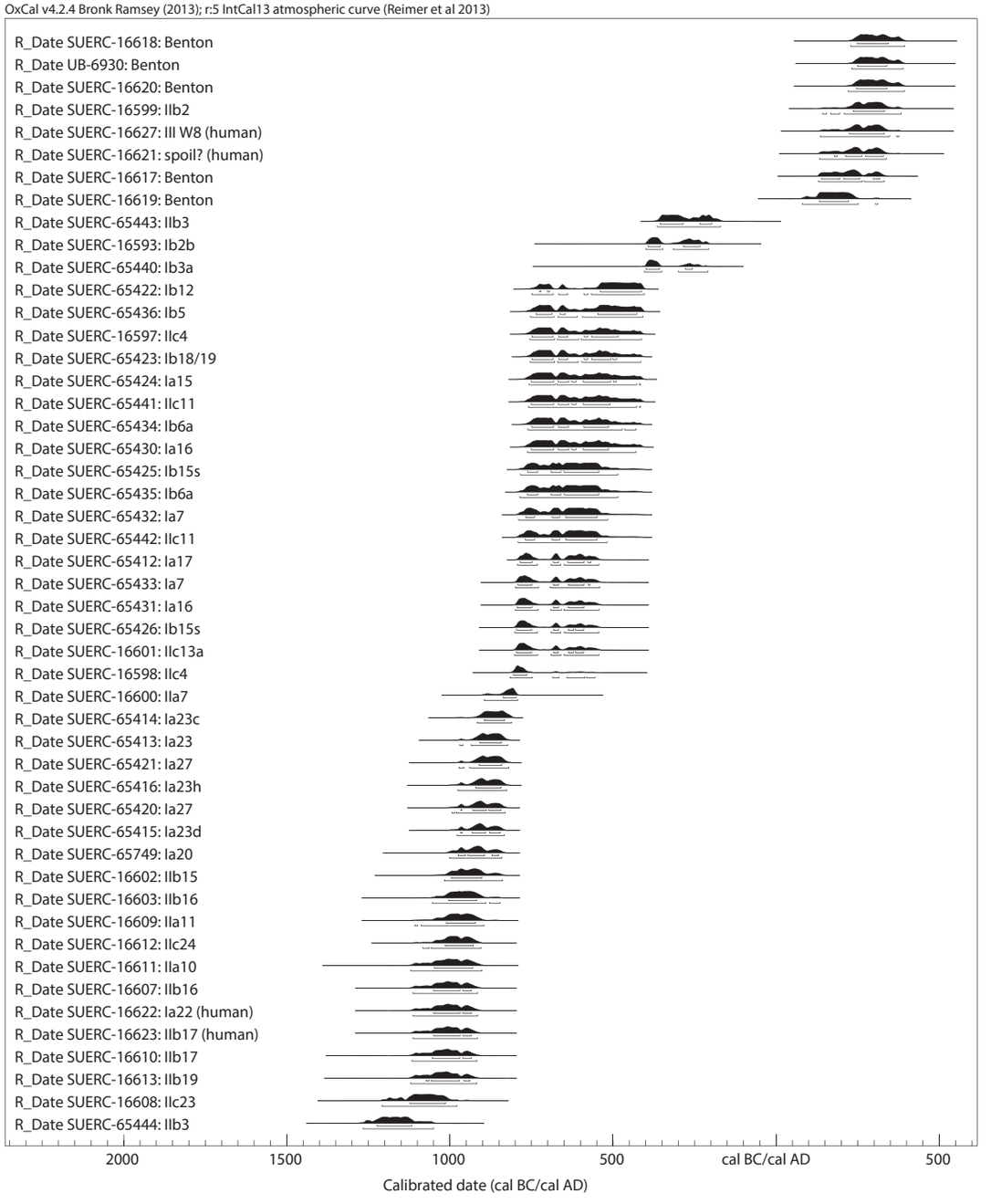

Illustration 4.1

Radiocarbon dates from the Sculptor's Cave plotted in date order. These appear to show broad continuity from the Late Bronze Age to the later centuries BC. The apparent hiatus in the last centuries BC/first centuries AD is likely to relate to the truncation of the upper deposits during Sylvia Benton's excavations. The later dates are from human bone excavated from these 'lost' deposits

Sample selection was hampered by the biases of preservation within different parts of the cave stratigraphy. Large quantities of carbonised organic material (charred cereal grains, hazelnut shell etc) survived from the lower levels (having been rediscovered during the course of the recent post-excavation programme). However, in the upper parts of the sequence, the few surviving charred grains were too sparse to be reliably interpreted as relating to contemporary deposition. There was however sufficient animal bone present to indicate continued deposition of food debris throughout the sequence. Given the nature of deposition and limitations of preservation, the following priority system for dating was adopted:

Table 4.1
Radiocarbon dates from the Sculptor's Cave. *Result calibrated using Marine13

Lab ID	Context	Block	Context description	Material	Species	Element	$\delta^{13}C$ (‰)	$\delta^{15}N$ (‰)	C:N	Radiocarbon age (BP)	Calibrated date (95% confidence)
SUERC-16593	Ib2b	1.7	Articulated dog burial	Bone	*Canis familiaris*	Radius	–21.3	9.0	3.3	2265±35	400–200 cal BC
SUERC-16597	IIc4	2.7	Thick deposit of soft silty clay	Bone	*Bos taurus*	Femur	–22.2	6.0	3.6	2455±30	770–410 cal BC
SUERC-16598	IIc4	2.7	Thick deposit of soft silty clay	Bone	Ovicaprid	Tibia	–21.7	6.1	3.5	2580±35	810–670 cal BC
SUERC-16599	IIb2	2.7	Thick deposit of soft silty clay	Bone	*Sus scrofa*	Radius	–22.3	7.1	3.4	1760±35	cal AD 140–390
SUERC-16600	IIa7	2.6	Burnt deposit	Bone	*Bos taurus*	Radius	–22.2	7.2	3.5	2565±35	900–790 cal BC
SUERC-16601	IIc13a	2.5	Lens of charcoal	Bone	Ovicaprid	Metatarsal	–21.0	5.8	3.2	2545±35	810–540 cal BC
SUERC-16602	IIb15	2.4	Laminated sands and fine silts	Bone	*Bos taurus*	Scapula	–22.4	7.4	3.5	2790±35	1020–840 cal BC
SUERC-16603	IIb16	2.3	Thick (0.2m) deposit of silty clay	Bone	Ovicaprid	Thoracic vertebra	–22.3	4.4	3.3	2810±35	1050–850 cal BC
SUERC-16607	IIb16	2.3	Thick (0.2m) deposit of silty clay	Bone	Ovicaprid	Long bone	–22.1	9.5	3.3	2845±35	1120–910 cal BC
SUERC-16608	IIc23	2.2	Laminated sands and fine silts	Bone	*Bos taurus*	Femur	–21.7	5.7	3.5	2895±35	1210–970 cal BC
SUERC-16609	IIa11	2.2	Laminated sands and fine silts	Bone	Ovicaprid	Femur	–22.2	4.1	3.2	2820±35	1060–890 cal BC
SUERC-16610	IIb17	2.2	Laminated sands and fine silts	Bone	*Sus scrofa*	Tibia	–22.3	6.4	3.2	2850±35	1120–910 cal BC
SUERC-16611	IIa10	2.1	Mid-brown sandy clay	Bone	*Bos taurus*	Scapula	–22.4	4.7	3.3	2840±40	1120–900 cal BC
SUERC-16612	IIc24	2.2	Hard-packed 'trampled' layer	Bone	Ovicaprid	Long bone	–21.8	7.7	3.3	2830±30	1060–900 cal BC
SUERC-16613	IIb19	2.1	Laminated sands	Bone	Caprine	Femur	–21.8	9.2	3.2	2855±35	1130–910 cal BC
SUERC-16617	Benton	n/a	No contextual information	Bone	*Homo sapiens*	Axis vertebra (CV2)	–21.1	10.0	3.1	1795±35	cal AD 120–340
SUERC-16618	Benton	n/a	No contextual information	Bone	*Homo sapiens*	Axis vertebra (CV3)	–22.0	10.8	3.2	1735±35	cal AD 220–400

Lab ID	Context	Block	Context description	Material	Species	Element	$\delta^{13}C$ (‰)	$\delta^{15}N$ (‰)	C:N	Radiocarbon age (BP)	Calibrated date (95% confidence)
SUERC-16619	Benton gnd square D7	n/a	No contextual information	Bone	*Homo sapiens*	Axis vertebra (CV5)	–21.0	11.0	2.9	1835±35	cal AD 80–320
SUERC-16620	Benton gnd square B4	n/a	No contextual information	Bone	*Homo sapiens*	Axis vertebra (CV6)	–21.4	11.0	3.2	1740±35	cal AD 220–400
SUERC-16621	Spoil heap erosion	n/a	Eroding from spoil at front of cave: likely from Benton's excavations	Bone	*Homo sapiens*	Tibia (right) (SF1100)	–20.9	10.4	3.1	1780±35	cal AD 130–350
SUERC-16622	IIb16/17	2.3	Thin lens of clay	Bone	*Homo sapiens*	Mandible (SF235)	–21.2	10.6	3.3	2845±35	1120–910 cal BC
SUERC-16623	IIb17	2.2	Laminated sands and fine silts	Bone	*Homo sapiens*	Mandible (SF225)	–21.5	11.3	3.5	2845±35	1120–910 cal BC
SUERC-16627	III	n/a	Unstratified	Bone	*Homo sapiens*	Thoracic vertebra (SF1101)	–21.3	11.2	3.0	1770±35	cal AD 130–380
SUERC-65412	Ia17	1.3	Sandy surface	Carbonised nutshell	*Corylus avellana*	n/a	–24.0	n/a	n/a	2522±26	800–540 cal BC
SUERC-65749	Ia20	1.2	Sand deposit	Carbonised cereal	*Hordeum vulgare* var. *nudum*	n/a	–22.2	n/a	n/a	2775±30	1010–830 cal BC
SUERC-65413	Ia23	1.2	Sand layer	Carbonised cereal	*Hordeum* sp.	n/a	–23.8	n/a	n/a	2744±26	970–820 cal BC
SUERC-65414	Ia23c	1.2	Clay deposit	Carbonised cereal	*Hordeum vulgare* var. *vulgare*	n/a	–25.0	n/a	n/a	2720±29	930–810 cal BC
SUERC-65415	Ia23d	1.2	Charcoal surface	Carbonised nutshell	*Corylus avellana*	n/a	–23.8	n/a	n/a	2764±26	980–830 cal BC
SUERC-65416	Ia23h	1.2	Sand lens	Carbonised cereal	*Hordeum vulgare* var. *nudum*	n/a	–23.3	n/a	n/a	2754±29	980–820 cal BC
SUERC-65420	Ia27	1.1	Trampled surface	Carbonised nutshell	*Corylus avellana*	n/a	–24.2	n/a	n/a	2762±29	1000–830 cal BC
SUERC-65421	Ia27	1.1	Trampled surface	Carbonised nutshell	*Corylus avellana*	n/a	–25.3	n/a	n/a	2745±29	980–820 cal BC
SUERC-65422	Ib12	1.4	Charcoal layer	Carbonised cereal	*Hordeum vulgare* var. *nudum*	n/a	–25.7	n/a	n/a	2429±29	750–400 cal BC
SUERC-65423	Ib18/19	1.3	Sand and clay laminae	Carbonised cereal	*Hordeum vulgare* var. *vulgare*	n/a	–24.6	n/a	n/a	2457±26	770–400 cal BC
SUERC-65424	Ia15	1.3	Sand and clay laminae	Bone	Large terrestrial mammal	Mandible	–21.5	7.0	3.2	2460±34	770–400 cal BC

Lab ID	Context	Block	Context description	Material	Species	Element	$\delta^{13}C$ (‰)	$\delta^{15}N$ (‰)	C:N	Radiocarbon age (BP)	Calibrated date (95% confidence)
SUERC-65425	Ib15s	1.4	Cobbled surface	Bone	*Sus scrofa*	Femur	–21.1	6.5	3.2	2488±33	790–430 cal BC
SUERC-65426	Ib15s	1.4	Cobbled surface	Bone	*Ovis aries*	Ulna	–21.1	5.8	3.2	2543±34	800–540 cal BC
SUERC-65430	Ia16	1.5	Loamy deposit	Bone	*Bos taurus*	Mandible	–21.2	5.9	3.2	2464±31	770–410 cal BC
SUERC-65431	Ia16	1.5	Loamy deposit	Bone	Medium terrestrial mammal	Sacrum	–21.9	5.9	3.2	2539±34	800–540 cal BC
SUERC-65432	Ia7	1.5	Thick mixed deposit	Bone	Medium terrestrial mammal	Long bone	–22.5	6.5	3.2	2502±34	800–510 cal BC
SUERC-65433	Ia7	1.5	Thick mixed deposit	Bone	*Ovis aries*	Metatarsal	–21.5	7.2	3.2	2534±34	800–540 cal BC
SUERC-65434	Ib6a	1.6	Burnt cobbles and ash	Bone	*Bos taurus*	2nd phalanx	–21.9	7.1	3.3	2463±26	770–410 cal BC
SUERC-65435	Ib6a	1.6	Burnt cobbles and ash	Bone	Medium terrestrial mammal	Long bone	–21.6	7.1	3.3	2489±34	790–430 cal BC
SUERC-65436	Ib5	1.6	Mixed sandy deposit	Bone	*Ovis aries*	Mandible	–21.9	8.3	3.2	2444±33	770–400 cal BC
SUERC-65440	Ib3a	1.7	Degraded sandstone deposit	Bone	Large terrestrial mammal	Long bone	–22.3	6.4	3.2	2283±33	410–230 cal BC
SUERC-65441	IIc11	2.6	Sand and silt laminae	Bone	Large terrestrial mammal	Long bone	–21.7	6.7	3.2	2461±33	770–410 cal BC
SUERC-65442	IIc11	2.6	Sand and silt laminae	Bone	Small/medium terrestrial mammal	Rib	–21.6	7.6	3.2	2504±34	800–510 cal BC
SUERC-65443	IIb3	2.8	Ash and sand laminae	Bone	Medium terrestrial mammal	Rib	–21.9	4.4	3.2	2189±33	370–160 cal BC
SUERC-65444	IIb3	2.8	Ash and sand laminae	Bone	Medium/large terrestrial mammal	Humerus	–22.7	6.4	3.2	2958±34	1270–1050 cal BC
SUERC-65445	Ia/Ib baulk	n/a	Interface between natural clay and laminated sands in West Passage	Bone	*Phalacrocoracidae* (cormorant family)	Tibiotarsus	–12.5	16.4	3.3	3284±34	*1380–970 cal BC
SUERC-68717	Spoil heap (2014)	n/a	Spoil at front of cave: likely from Benton's excavations	Bone	*Homo sapiens*	Left temporal (SF1130) (aDNA: male)	–21.7	11.0	3.2	1696±29	cal AD 250–420
UB-6930	Benton gnd square D4	n/a	No contextual information	Bone	*Homo sapiens*	Axis vertebra (CV4)	–20.9	11.5	2.9	1738±33	cal AD 230–400

1. The preferred sample type was individual charred cereal grains from contexts in which such grains were sufficiently numerous to suggest that the grain was incorporated into accumulating deposits shortly after burning.
2. Where charred cereal grains were not available, charred hazelnut shells were selected from contexts in which they were sufficiently numerous to suggest that they were incorporated into accumulating deposits shortly after burning. In one case, hazelnut shell was preferentially selected, despite the presence of charred grains, because of the very large concentration of hazelnuts in that particular context (Ia17; SUERC-65412).
3. Where the preferred materials were unavailable, bone deriving from large and medium terrestrial mammals was selected. All the available mammal bone was disarticulated and there was not, therefore, the opportunity to select articulated material. The animal bone was, however, well preserved, with good surface integrity. To aid the identification of any potential residuality within this material, wherever possible, two paired samples were selected from each context: where possible, these paired samples were from separate species or, where this was not possible, from different individuals as identified by size. Wherever possible, bones from identified species were submitted but, in a few cases, identification was only possible to the level of large or medium terrestrial mammal. Since no evidence for residuality was identified in the 2006/7 dating programme, it was possible to have some confidence that this would not be a major issue.
4. A single seabird bone was selected from the junction of natural sand and clay deposits underlying the anthropogenic deposits.

4.1.5 Additional sample: 2016

In 2016, the opportunity was taken to obtain a further determination as part of the GenScot Project, investigating the ancient DNA of selected individuals from prehistoric Scotland (Armit et al 2016). A single left temporal bone (SF35/GenScot 69) retrieved from the excavation of Benton's spoil heap was selected. The result obtained is consistent with the date range of other Roman Iron Age human remains from the cave.

4.2 Results and calibration

All 50 samples submitted to SUERC were processed following methods outlined in Dunbar et al (2016) and were graphitised and measured following Naysmith et al (2010). The human bone dated at Queens University Belfast was pretreated according to methods outlined in Longin (1971) and Pearson (1984). The pretreated and freeze-dried QUB sample was placed in a quartz tube with a strip of silver ribbon to remove nitrates, chlorides and CuO; it was then sealed under vacuum and combusted to CO_2 overnight at 850°C. The CO_2 was converted to graphite on an iron catalyst using the zinc reduction method (Vogel et al 1984). The graphite sample was sent to the Oxford Radiocarbon Accelerator Unit (ORAU) where it was measured as described by Bronk Ramsey et al (2004). Both the SUERC and Belfast laboratories maintain continual programmes of quality assurance procedures, in addition to participation in international inter-comparisons (Scott 2003; Scott et al 2010). These tests indicate no laboratory offsets and demonstrate the validity of the measurements quoted.

The results of all 51 radiocarbon age determinations are presented in table 4.1, where they are quoted in accordance with the Trondheim Convention (Stuiver and Kra 1986) as conventional radiocarbon ages (Stuiver and Polach 1977). Calibrated date ranges were calculated using the calibration curves of Reimer et al (2013) and OxCal v4.2 (Bronk Ramsey 1995; 1998; 2001; 2009). The terrestrial calibration curve, IntCal13, was used for all samples, with the exception of the sample on a seabird bone, which was calibrated using Marine13. The simple calibrated dates are cited in the text, both here and in other chapters, at 95% confidence, and quoted with the end points rounded outwards to 10 years. Ranges quoted in italics are posterior density estimates derived from mathematical modelling of archaeological problems (below). Ranges in plain type have been calculated according to the maximum intercept method (Stuiver and Reimer 1986). All other ranges are derived from the probability method (Stuiver and Reimer 1993).

4.3 Methodological approach

A Bayesian approach has been applied to the interpretation of the Sculptor's Cave chronology (Buck et al 1996). Although simple calibrated dates are accurate estimates of the age of samples, this is not usually what archaeologists really wish to know. It is the dates of the archaeological events represented by those samples that are of interest. At the Sculptor's Cave, for example, it is the dating and duration of activity in the East and West Passages, rather than the dates of individual samples per se, that are of interest. The chronology of this activity can be estimated not only by using the absolute dating from the radiocarbon measurements but also by deploying the stratigraphic relationships between samples and the relative dating information provided by the archaeological phasing.

Methodology is now available which allows the combination of these different types of information explicitly, producing realistic estimates of the dates of archaeological interest. It should be emphasised that the posterior density estimates produced by this modelling are not absolute. Rather, they are interpretative estimates, which can and will change as further data become available and as other researchers choose to model the existing data from different perspectives. The technique used is a form of Markov Chain Monte Carlo sampling and has been applied using the program OxCal v4.2 (http://c14.arch.ox.ac.uk/). Details of the algorithms employed by this program are available in Bronk Ramsey (1995; 1998; 2001; 2009) or from the online manual. The algorithm used in the model can be derived from the OxCal keywords and bracket structure shown in illus 4.2.

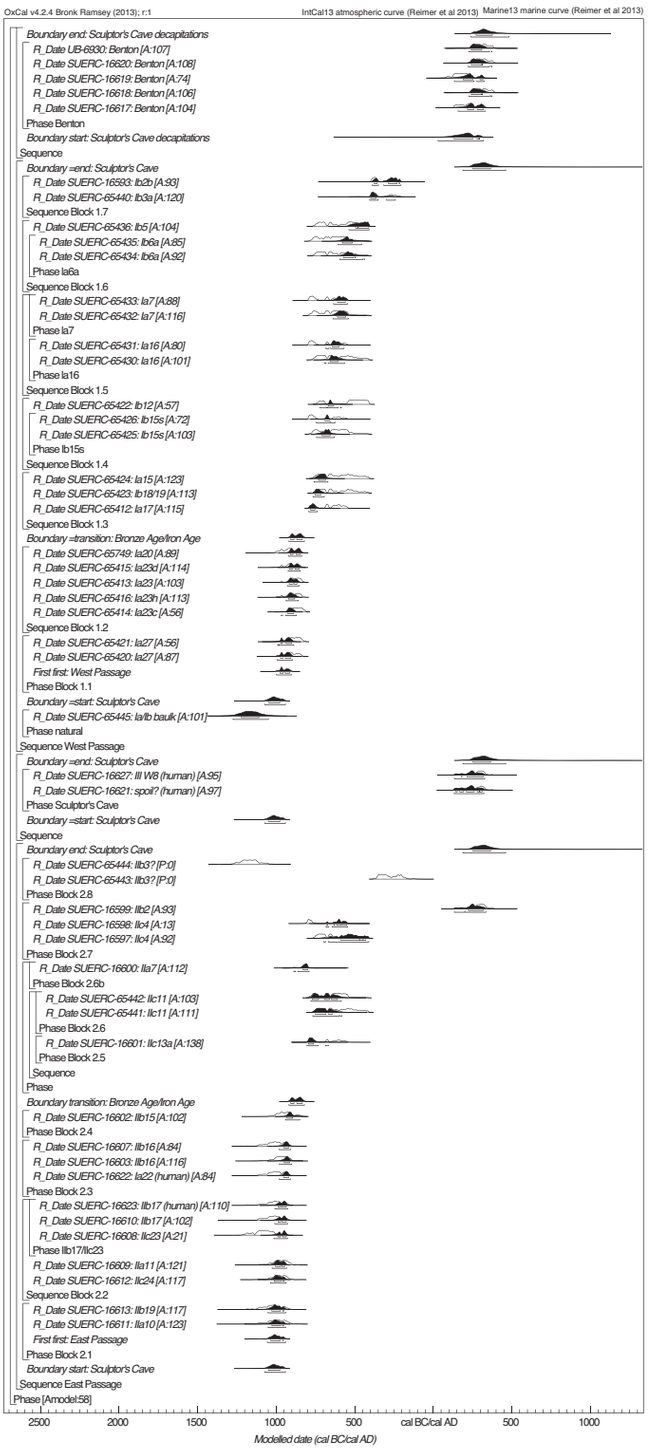

Illustration 4.2

Chronological model for the excavated activity at Sculptor's Cave. Each distribution represents the relative probability of an archaeological event. The distributions in outline show the calibration of each result by the probability method (Stuiver and Reimer 1993). The solid distributions are *posterior density estimates* derived from the chronological model. This model is exactly defined by the square brackets and OxCal keywords at the left of the diagram

4.4 Samples and models

The chronological model was developed to answer a series of questions:

- What are the overall start and end dates for human activity in the cave?
- What is the temporal relationship of the deposition of human remains in the East and West Passages? Did human activity within the excavated deposits begin in one passage before the other?
- Does the dating evidence demonstrate continuity or discontinuity in the accumulation of deposits in the entrance passages?

Additional queries were also made of the model:

- Is it possible that the vertebrae showing signs of decapitation are indicative of a single event?
- Can we estimate the time elapsed between the beginning of natural clay formation in the cave (immediately overlying the seabird bone) and the beginning of human activity?
- What were the start and end dates and duration of the deposition of human remains in the Late Bronze Age?

To address these questions, the radiocarbon dates from the Sculptor's Cave were divided into three broad groups:

1. Samples that derived from stratified deposits in the East Passage.
2. Samples that derived from stratified deposits in the West Passage.
3. Unstratified remains recovered from the Benton human bone archive and the spoil heap outside the entrance to the cave.

4.4.1 East Passage

There are 20 radiocarbon dates from the East Passage (illus 4.3) that are stratified within 8 blocks. At the base of the sequence are two results (SUERC-16611, -16613) from a cattle scapula and goat femur in Block 2.1. This is followed by a stratified sequence of dates on material from within Block 2.2, beginning with a sheep/goat long bone shaft fragment (SUERC-16612), followed by a sheep/goat femur (SUERC-16609) and finally three results (SUERC-16608, -16610, -16623) on a cattle femur, pig tibia, and human mandible (SF225). Block 2.3 begins with a date from a human mandible (SF235; SUERC-16622) followed by two results (SUERC-16603, -16607) on a sheep/goat vertebra and long bone shaft fragment. Rounding out the Bronze Age layers is a single result (SUERC-16602) on a cattle scapula in Block 2.4.

The Iron Age layers in the East Passage begin with Block 2.5, from which there is a radiocarbon date (SUERC-16601) on a sheep/goat metatarsal. Two results (SUERC-65441, -65442) from the overlying Block 2.6 were made on a fragment of large terrestrial mammal long bone and a small/medium terrestrial mammal rib. A

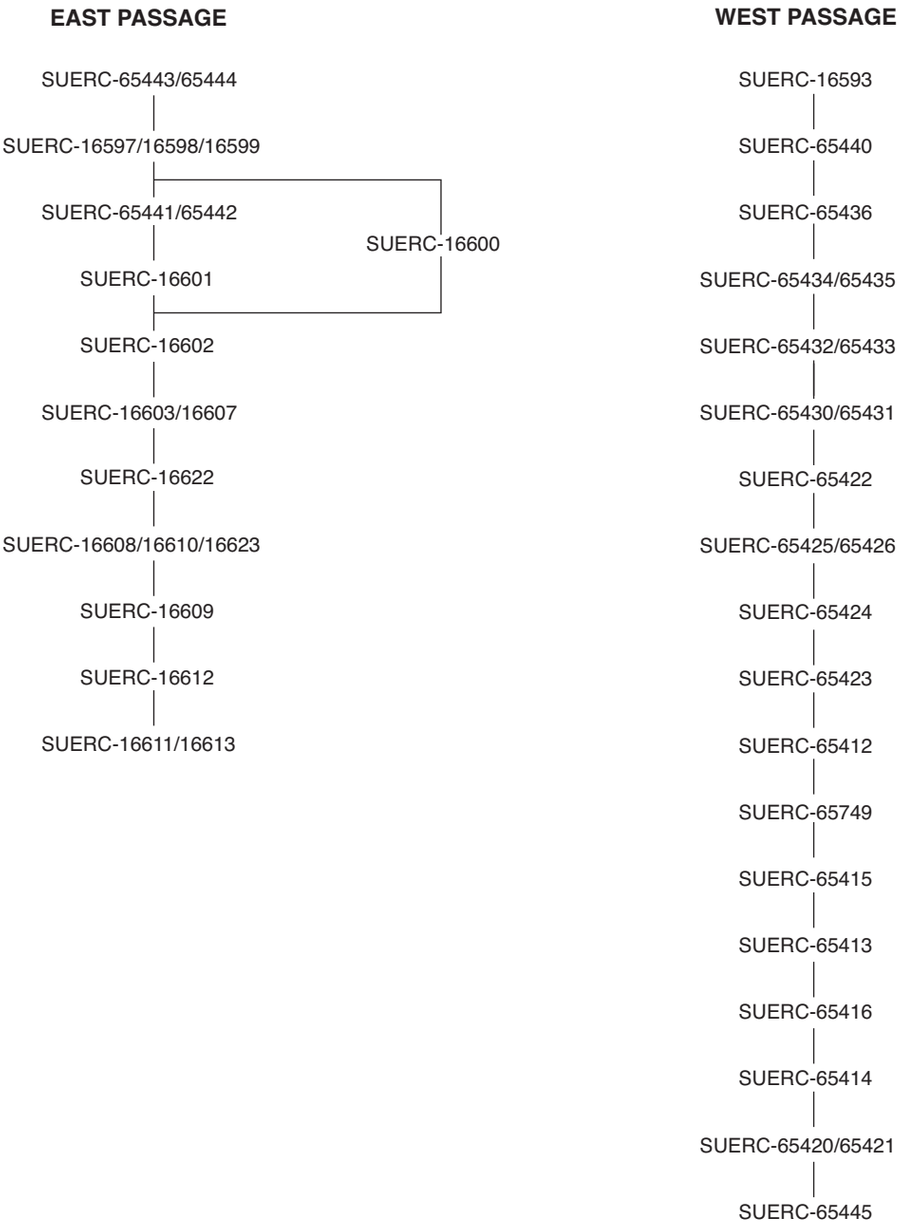

Illustration 4.3
Schematic showing stratigraphic relationships between AMS determinations

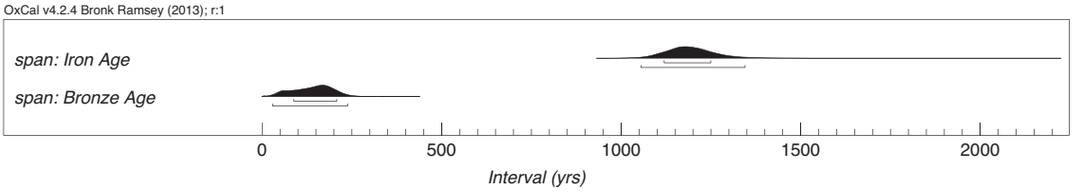

Illustration 4.4
The estimated span of activity in the Sculptor's Cave in the Bronze and Iron Ages, as modelled in illus 4.2

third result (SUERC-16600), on a cattle radius, also derives from Block 2.6, although stratigraphically it could be argued equally to sit alongside deposits in Block 2.5; the model could associate it with either block but it remains assigned, on interpretive grounds, to Block 2.6. Block 2.7 was very thick and combines individual layers that were not excavated separately by the Shepherds. There are three results (SUERC-16597, -16598, -16599) on a cattle femur, sheep/goat tibia and pig radius. From the final Block 2.8 there are two results (SUERC-65443, -65444) from a medium terrestrial mammal rib and a medium/large terrestrial mammal humerus.

4.4.2 West Passage

There are a total of 22 radiocarbon dates from 7 excavated blocks of anthropogenic deposits in the West Passage and an additional date (SUERC-65445) on a tibiotarsus from a seabird of the cormorant family that was recovered from the interface between the underlying natural clay and gravel deposits (illus 4.3). From the Late Bronze Age levels there are two dates (SUERC-65420, -65421) on single fragments of carbonised hazelnut shell in Block 1.1, which are followed by 5 dates in stratigraphic sequence within Block 1.2. Most of the dates come from charred plant material that was described as coming from discrete deposits and interpreted as belonging to separate events. At the base of the Block 1.2 sequence is a result (SUERC-65414) from a grain of barley, above which there are two further results (SUERC-65416, -65413) on barley grains from other sequential deposits. These three barley grains are followed by a result (SUERC-65415) on a charred hazelnut shell. The Late Bronze Age portion of the sequence is capped by a result (SUERC-65749) on a further barley grain.

From Block 1.3, there are three results (SUERC-65412, -65423, -65424) in sequence, from lowest to highest, on a charred hazelnut shell, carbonised barley grain and large terrestrial mammal mandible fragment. Block 1.4 has three results: SUERC-65425 and -65426 are on a pig femur and sheep/goat ulna, overlain by a deposit from which a charred barley grain was dated (SUERC-65422). Block 1.5 has four results: two paired dates (SUERC-65430, -65431) on a cattle mandible and medium terrestrial mammal sacrum and a further pair (SUERC-65432, -65433) on a medium terrestrial mammal long bone shaft fragment and a sheep/goat metatarsal from an overlying deposit. The three results from Block 1.6 are from two levels, with two dates (SUERC-65434, -65435) on a calf phalanx and medium terrestrial mammal long bone shaft fragment from the lower level, and a result (SUERC-65436) from a sheep/goat mandible from the upper level. The Iron Age portion of the sequence finishes with two dates (SUERC-65440, -16593) on a large terrestrial mammal long bone shaft fragment and dog radius in sequence in Block 1.7.

4.4.3 Unstratified remains

There are eight results on unstratified human remains from the Sculptor's Cave. Three results (SUERC-16621 -16627, -68717) are from a tibia shaft, a thoracic vertebra and a left temporal. The tibia was recovered from the surface of the Benton spoil heap outside the cave entrance, the thoracic vertebra was excavated from disturbed remains in Area III (section 2.1.5; illus 2.6) and the temporal bone was recovered from Benton's spoil heap during the 2014 excavations (box section 2). The remaining five results (SUERC-16617, -16618, -16619, -16620, UB-6930) are all from cervical vertebrae that present evidence for decapitation.

4.4.4 The model

The chronological model developed stipulates that all of the material recovered from the anthropogenic deposits belongs to one of two phases of activity – Late Bronze Age or Iron Age – and that these two phases are sequential but not necessarily contiguous. This allows for calculation of the overall start and end dates of activity in the cave as well as dates for the end of the Late Bronze Age activity and beginning of the Iron Age activity. It also enables a determination of whether the dating supports a hiatus in the activity. Although subtle and subjective, there is a change from fairly thin deposits of sands and clays to thick deposits of looser material with hearth debris that the Shepherds took to mark the end of Late Bronze Age activity. This transition can be identified in the East Passage at the boundary between Blocks 2.4 and 2.5 and in the West Passage at the boundary between Blocks 1.2 and 1.3.

Before commencing with the modelling, it was noticed that the two results (SUERC-65443 and -65444) from East Passage Block 2.8 are from the second or first millennia cal BC and are approximately 1000 years different in date. The earlier date (SUERC-65444) is certainly residual and has been excluded from all modelling. However, it remains difficult to reconcile the first-millennium cal BC date (SUERC-65443) in Block 2.8 when there is a second- to third-century cal AD date (SUERC-16599) immediately below in Block 2.7. Since we know that there was modern disturbance both by Benton and by subsequent informal digging in the cave, the later date (SUERC-65443) from Block 2.8 is also excluded from all modelling. It appears likely, on the basis of the radiocarbon dates, that the deposits of Block 2.8 should be regarded as highly disturbed.

The five results representing decapitated individuals were modelled as a separate phase of activity that can be independently compared to the stratified sequence from the Shepherd excavations.

4.5 Model results

The model has low agreement (Amodel=58) between the radiocarbon dates and the recorded stratigraphic relationships between samples. The depth of the recorded stratigraphy and high number of samples is almost certainly the cause of the overall agreement dipping just below the usual threshold of 60. Given the results of the sensitivity analysis (section 4.5.1), this model should be considered robust. The model estimates that activity in the Sculptor's Cave began in *1075–940 cal BC* (*95% probability*; illus 4.2, *start: Sculptor's Cave*) and probably in *1050–975 cal BC* (*68% probability*). Bronze Age activity spanned *35–240 years* (*95% probability*; illus 4.4, *span: Bronze Age*) and probably *85–210 years* (*68% probability*). The Bronze Age activity ended in *920–820 cal BC* (*95% probability*; illus 4.2, *transition: Bronze Age/Iron Age*) and probably in either *910–885 cal BC* (*26% probability*) or *870–830 cal BC* (*43% probability*). Activity in the Sculptor's Cave ended in

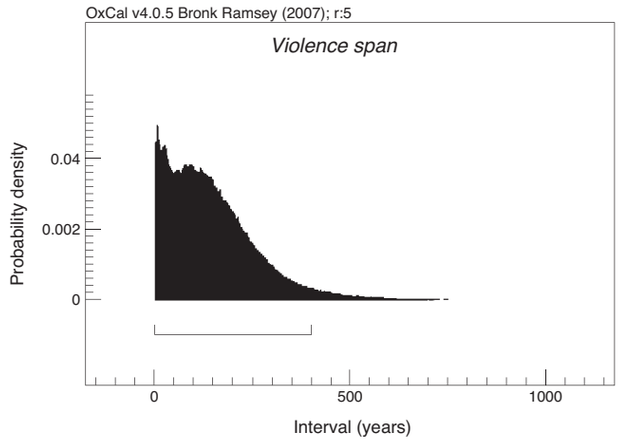

Illustration 4.5
The estimated span of the five cut-marked vertebrae, as modelled in illus 4.2

cal AD 240–485 (*95% probability*; illus 4.2, *end: Sculptor's Cave*) and probably in *cal AD 270–380* (*68% probability*). The Iron Age activity was long-lived and spanned *1055–1345 years* (*95% probability*; illus 4.4, *span: Iron Age*) and probably *1120–1250 years* (*68% probability*).

The human cervical vertebrae that exhibit signs of decapitation have radiocarbon ages that are statistically consistent (T'=6.6; ν=4; T'(5%)=9.5; Ward and Wilson 1978). This indicates that they could be the same age, with the individuals represented dying in the same 'event' (illus 4.5). If these five people were decapitated at the same time, the calibrated weighted mean of those ages suggests the event occurred in *cal AD 220–340* (*95% probability*), probably *cal AD 240–260* (*27% probability*) or *cal AD 285–290* (*4% probability*) or *cal AD 295–325* (*37% probability*) (illus 4.6). However, it is possible that the cave was used periodically for carrying out beheadings and, if this was the case, then this activity is estimated to have begun in *cal AD 30–320* (*95% probability*; illus 4.2, *start: Sculptor's Cave decapitations*) and probably in either *cal AD 130–255* (*63% probability*) or *cal AD 275–295* (*5% probability*). The activity persisted for *0–410 years* (*95% probability*; illus 4.5, *span: Sculptor's Cave decapitations*) and probably *0–190 years* (*68% probability*). The decapitations ended in *cal AD 240–485* (*95% probability*; illus 4.2, *end: Sculptor's Cave decapitations*) and probably in *cal AD 270–380* (*68% probability*).

4.5.1 Sensitivity analysis

The sensitivity analysis was used to explore the impact of the stratigraphy within the blocks to the model output, as the Primary model contained many vertical links between individual samples through the stratigraphy that could lead to over constraint in the model. The only difference between the Primary model and this Alternative model was the removal of sequencing within individual blocks, allowing the radiocarbon dates associated with each of them to be unordered. The Alternative model has good agreement between the dates and the model assumptions (Amodel=63). The date estimates for the start and end of activity at the Sculptor's Cave and the transition between the Bronze Age and Iron Age phases differ in range by 5–20 years when comparing the 95% probability ranges, and less when comparing the 68% probability ranges. This demonstrates the overall robustness of the Primary model, which is the preferred model used to address further queries.

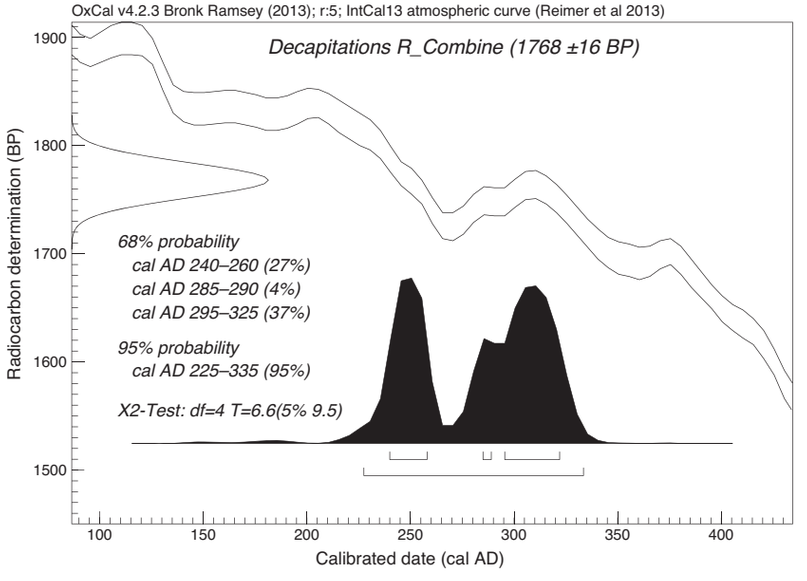

Illustration 4.6
The estimated date for the five cut-marked vertebrae if they occurred as part of a single event. The radiocarbon ages have been combined prior to calibration to form a weighted mean (Ward and Wilson 1978)

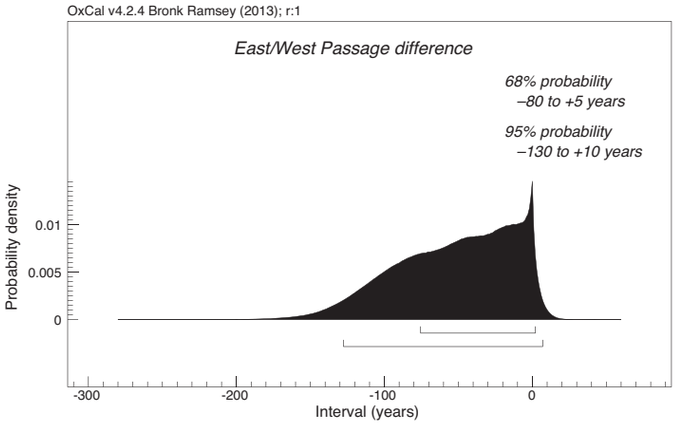

Illustration 4.7
The difference between the earliest deposit in the East and West Passages, as modelled in illus 4.2

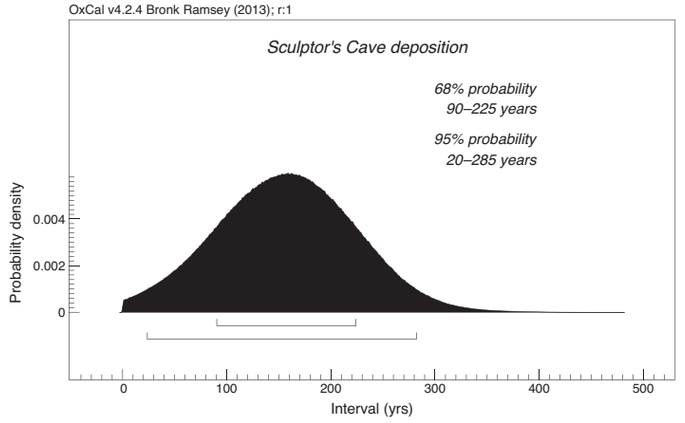

Illustration 4.8
The hiatus in time between the deposition of the seabird bone (SUERC-65445) and the start of human activity in the Sculptor's Cave (*start: Sculptor's Cave*), as modelled in illus 4.2

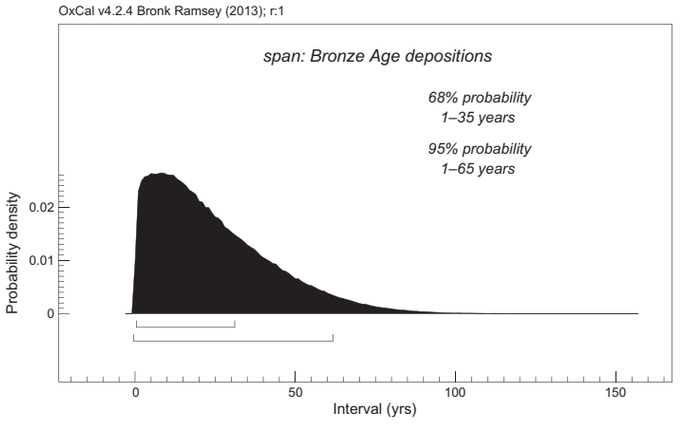

Illustration 4.9
The span of time for Bronze Age human deposition in the Sculptor's Cave, as modelled in illus 4.2

4.5.2 Further queries of the Primary model

The chronological model can be used for more than simply producing estimates for the start, end and duration of dated activity at a site. The resulting model can be queried to determine the temporal relationship between dated events (eg the order of two events), the hiatus between two dated events, or even to explore the relationship between events dated at two different sites. The remaining questions from above (section 4.4) are addressed here:

1. What is the temporal relationship between the excavated deposits in the East and West Passages? By calculating and comparing the probabilities for the 'first' depositional event in both the East and West Passages (though see section 2.3.4), the model suggests that there is a 95% probability that deposition began in the East Passage. The difference between these two probabilities is between *–130 and 10 years* (*95% probability*; illus 4.7), or *–80 and 5 years* (*68% probability*).
2. Can we estimate the time elapsed between the beginning of sand formation in the cave that contained the seabird bone and the beginning of human activity? Similar to the query above, it is possible to estimate the amount of time that elapsed between the deposition of the seabird bone (SUERC-65445) and the start of human activity in the cave (*start: Sculptor's Cave*). This calculation is *20–285 years* (*95% probability*; illus 4.8, *Sculptor's Cave deposition*) or probably *90–225 years* (*68% probability*).
3. What were the start and end dates and duration of the deposition of human remains in the Late Bronze Age? There are two dates on Late Bronze Age human depositions in the cave (SUERC-16622 and -16623). The dates on the two samples provide the start and end. *SUERC-16623: IIb17 (human)*, from Block 2.2, has a modelled date of death and deposition in *1010–925 cal BC* (*95% probability*; illus 4.2) and probably in either *990–970 cal BC* (*23% probability*) or *965–935 cal BC* (*45% probability*). *SUERC-16622: Ia22 (human)* is from Block 2.3 and has an estimated date of *985–905 cal BC* (*95% probability*; illus 4.2) and probably *955–920 cal BC* (*68% probability*). The difference between the dates provides an estimated span of *1–65 years* (*95% probability*; illus 4.9, *span: Bronze Age depositions*) and probably *1–35 years* (*68% probability*).
4. Does the dating evidence demonstrate continuity or discontinuity in the accumulation of deposits in the entrance passages? While the dating from the Sculptor's Cave might be taken to suggest a discontinuity in deposition, with a hiatus of perhaps 400–500 years – between, on the one hand, the later first-millennium cal BC material in the upper levels of both the East and West Passages and the earlier first-millennium cal AD material in Block 2.7 of the East Passage and, on the other, the various human remains from Benton's spoil heap and decapitations – Benton had removed upper deposits from both passages and so the paucity of dates before the

decapitation 'event' might reasonably be a by-product of the material remaining after her intervention.

4.6 Discussion

Many of the implications of the Bayesian analysis of the radiocarbon dates are explored elsewhere in the relevant chapters, but it is useful to summarise some of the main features here.

The Bayesian model supports the archaeological interpretation, advanced in chapter 2, that deposition at the Sculptor's Cave was more or less continuous (if low in intensity) from its beginnings in the Late Bronze Age through to at least the later first millennium BC. The removal of the upper deposits throughout the entire cave by Sylvia Benton prevents any meaningful interrogation of possible continuity after this period, but the Late Roman Iron Age dates for many of the human remains and for significant parts of the artefact assemblage (see chapters 5 and 6) are suggestive. Despite the evidence for continuity, the deposition of human remains (for which the cave is so well known) appears confined to two potentially rather brief episodes separated by more than a millennium. The implications of this will be discussed in chapter 8.

The AMS dates have been useful in confirming the generally low level of residuality throughout much of the depositional sequence while highlighting the specific difficulties associated with the uppermost surviving deposits (notably Block 2.8). This has informed the interpretations of the formation processes within the cave advanced in chapter 2.

In relation to the dating of the Late Roman Iron Age decapitations, it is interesting to compare the results of Bayesian modelling to the sparse historical record of the period. If, as seems likely, the multiple decapitations do relate to a single event (illus 4.5), then it is probable that they were related in some way to the political and/or military events of the time (see discussion in chapter 8). Bayesian modelling suggests that they are unlikely to relate to the period of the Severan campaigns against the Maetae and Caledonii in AD 211. However, it is not impossible that they do relate in some way to the next documented Roman military incursion: the invasion of Constantinius Chlorus in AD 305, which falls within the 68% confidence range. It is entirely possible of course that the putative event relates to indigenous conflicts within the region, or even to undocumented conflict with the Roman army.